Cosmic Ray Flux Measurement with AMANDA-II

Dmitry Chirkin[1] for the AMANDA Collaboration[2]
(1) University of California at Berkeley, Berkeley, CA 94720, USA
(2) complete author list in G.C. Hill et al., these proceedings

Abstract

AMANDA-II is a neutrino telescope composed of 677 optical sensors organized along 19 strings buried deep in the Antarctic ice cap. It is designed to detect Cherenkov light produced by cosmic-ray- and neutrino-induced muons. The majority of events recorded by AMANDA-II are caused by muons which are produced in the atmosphere by high-energy cosmic rays. The leading uncertainties in simulating such events come from the choice of the high-energy model used to describe the first interaction of the cosmic rays, uncertainties in our knowledge and implementation of the ice properties at the depth of the detector, and individual optical module sensitivities. A method is developed that results in a flux measurement of cosmic rays with energies $1.5-200$ TeV per nucleon (95% of primaries causing low-multiplicity events in AMANDA-II have energies in this range) independent of ice model and optical module sensitivities. Predictions of six commonly-used high-energy interaction models - QGSJET, VENUS, NEXUS, DPMJET, HDPM, and SYBILL - are compared to data. Best agreement with direct measurements is achieved with QGSJET, VENUS, and NEXUS (preliminary: $\Phi_{0,\mathrm{H}} = 0.106 \pm 0.007$ $\mathrm{m}^{-2}\mathrm{s}^{-1}\mathrm{sr}^{-1}\mathrm{TeV}^{-1}$, $\gamma_{\mathrm{H}} = 2.70 \pm 0.02$).

1. Introduction

In order to measure the cosmic ray flux with AMANDA-II (Antarctic Muon And Neutrino Detector Array) [8], comparison of data with the detector simulation is necessary. A power law energy spectrum of the cosmic ray components with relative abundances taken from [9] was assumed. Overall normalization and spectral index were varied to match experimental data with simulated data. CORSIKA [1] (versions 6.016 and 6.018) was used to generate muon flux at the ice surface from the assumed cosmic ray flux. Simulation was performed for six high-energy models available with CORSIKA. Muons were propagated through ice to and through the detector with MMC [2] (version 1.08). To generate Cherenkov photons and simulate AMANDA-II response, the detector simulation program AMASIM [6] (version 2.73.14) was used.

Special emphasis was put on minimizing systematic uncertainties. The systematic uncertainty due to change of atmospheric conditions has been estimated by comparing experimental and simulated data from several different periods during the year 2000. The uncertainty in the knowledge of the muon cross sections in ice is less than 1% [7]. Muon propagation algorithm and computational errors were estimated to be smaller than that [3]. The knowledge of the ice density profile and the depth of the optical modules (OM) introduces an error of less than 1 m, which contributes less than 1% to the uncertainty in muon propagation.

To minimize hardware uncertainties, the number of muon events seen at the depth of each of the OMs of the detector was calculated using the method described in [4]. The distribution of noise hits was determined from data uncorrelated with muon signal. This distribution is folded with the distribution of hits coming from observed Cherenkov photons emitted by muons inside the detector. To account for photons from muons passing close to a given OM which are possibly missed by that OM, the *efficiency* of that OM was determined by analyzing the signal in the surrounding OMs (i.e. in the OMs above and below the given OM). To calculate the number of muons seen by the detector, noise is subtracted and efficiency-governed missed signal is added to the signal produced by each OM. This method is most precise for the OMs located close to the center of the detector [4].

The largest uncertainties in the simulation chain come from the photon propagation and detector signal simulation. These were estimated to be 15% for absolute OM sensitivities and 20% for optical properties of ice. Two methods were developed [4] that attempt to make the flux measurement insensitive to these uncertainties. The following section discusses one of these methods.

2. Method

Suppose a flux of vertical muons with spectrum $\Phi = \Phi_0 \cdot E^{-\gamma}$ is propagated through ice, losing energy continuously according to $dE/dx = a + b \cdot E$. The number of OMs that record at least one hit is roughly proportional to the energy lost inside the detector (located at depths between h_1 and h_2):

$$N_{\text{ch}} \approx \int_{h_1}^{h_2} \frac{dE}{dx}(h)\rho dh = (a + bE) \int_{h_1}^{h_2} e^{-bh}\rho dh \tag{1}$$

where ρ is proportional to the vertical density of OMs and depends on the OM sensitivities and optical properties of the ice. This approximation is valid when the fraction of hit channels is small [4]. Solving (1) for $E(N_{\text{ch}})$ and inserting it into $\Phi = \Phi_0 \cdot E^{-\gamma}$ one gets

$$\Phi = \Phi_0 \cdot \begin{cases} \left(\frac{N_{\text{ch}} - a\rho A}{b\rho A}\right)^{-\gamma} \\ \left(\frac{N_{\text{ch}} + \rho C - a\rho B}{b\rho B}\right)^{-\gamma} \end{cases} \Rightarrow N_{\text{ch}} \cdot \frac{d(\log \Phi)}{dN_{\text{ch}}} = \begin{cases} \frac{-\gamma N_{\text{ch}}}{N_{\text{ch}} - a\rho A} \\ \frac{-\gamma N_{\text{ch}}}{N_{\text{ch}} + \rho C - a\rho B} \end{cases} \tag{2}$$

where A, B, and C are functions of a, b, h_1, and h_2. The upper expression is for muons going through the detector, and the lower one is for muons stopping inside. A change in slope occurs at $N_{ch,0}$ corresponding to $E_0 = (e^{bh_2} - 1) \cdot a/b$, which depends only on the geometrical configuration of the detector. Therefore, the number of events with N_{ch} above $N_{ch,0}$ can be used to get the total flux above E_0, i.e. to find the normalization constant Φ_0. On both sides of this N_{ch} the slope $N_{ch} \cdot d(\log \Phi)/dN_{ch}$ is proportional to γ. It can also be seen that it does not depend on the OM sensitivities or ice properties, since ρ cancels out.
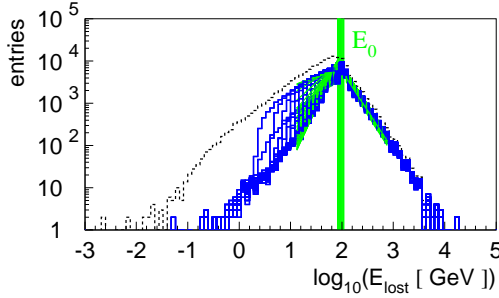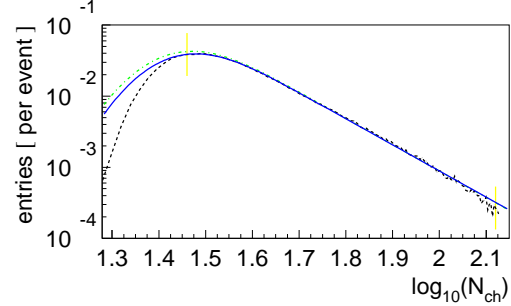

Fig. 1. Energy lost inside the detector

Fig. 2. N_{ch} distribution for OM 69

Fig. 1 shows the distribution of deposited energy E_{lost} for all muons seen by the detector (dashed histogram) and for muons passing through several horizontal layers in the detector (solid histograms). In the N_{ch} distribution (Fig. 2) the change in slope is more gradual than for E_{lost} and the slope itself is only well-defined above the break. The histogram (dashed line) is fit with

$$f(x) = \left(e^{p_1 + p_2 \cdot x}\right) \cdot \frac{1 - \mathrm{erf}\left(\frac{p_3 - x}{p_4}\right)}{2} \tag{3}$$

Solid line is for muons seen at the depth of OM closest to the center of the detector (69) and dot-dashed line is for all muons recorded by the detector. Different ice models result in somewhat different slopes. An ice-model-independent result can still be obtained by looking at the correlation of p_1 (normalization) and p_2 (spectral index correction) with p_3 (which is close to the location of the maximum in the N_{ch} distribution) (Fig. 3). Five empirical parabola fits corresponding to spectral index corrections of 0, ± 0.1, ± 0.2 (to values from [9]: $\gamma_H = 2.76$, $\gamma_{He} = 2.63$, etc.) are shown. Seven ice models lie close to their corresponding spectral index correction fits. Two ice models based on the measured ice properties are shown in black triangles, the rest use varied values for scattering, absorption and OM sensitivities. Experimental data (~ 2 hours from day 55, year 2000) are shown by solid circles. The results are stable even for significant changes in the detector configuration (conf.). Fig. 4 shows the result when one of the strings (1 through 19) is disabled, when an alternative cross-talk algorithm is used, and when the sensitivity of each OM is lowered by ≈ 40 %.
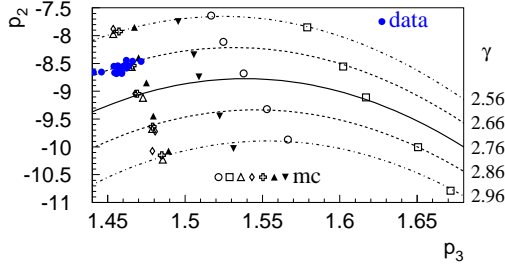
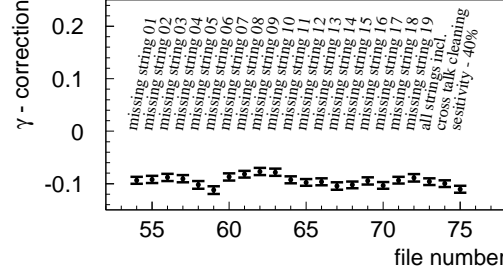**Fig. 3.** Correlation between p_2 and p_3

Fig. 4. Spectral index correction for data

3.   Results

The measured corrections apply to all cosmic ray components at $1.5-200$ TeV per nucleon. The values shown below are for hydrogen. Using QGSJET,

$$\gamma = 2.76(\text{H}) - 0.063 \pm 0.007(\text{ice}) \pm 0.014(\text{atm}) \pm 0.009(\text{conf}) = 2.70 \pm 0.02$$
$$\Phi_0 = 0.1057(\text{H}) + 0.000 \pm 0.002(\text{ice}) \pm 0.004(\text{atm}) \pm 0.006(\text{conf}) = 0.106 \pm 0.007$$

Direct measurements ($\gamma = 2.76 \pm 0.02$, $\Phi_0 = 0.1057 \pm 0.0003$ [9]; or more recently $\gamma = 2.71 \pm 0.02$, $\Phi_0 = 0.0873 \pm 0.0007$ [5]) agree best with QGSJET, NEXUS, and VENUS results of this paper.
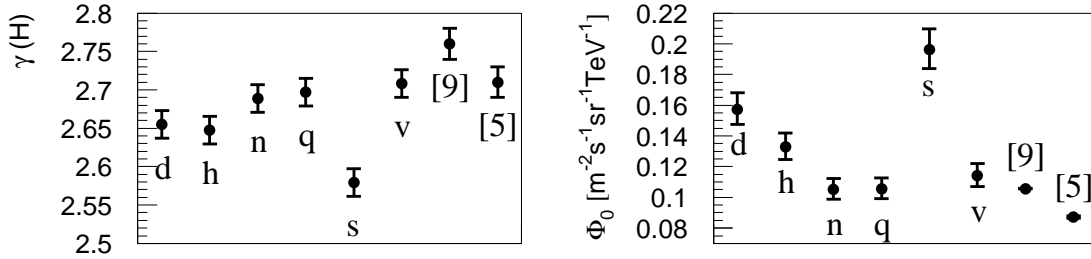

Fig. 5. Results for DPMJET, HDPM, NEXUS, QGSJET, SYBILL, VENUS (for H)
(preliminary)

4.   References

1. Chirkin, D., Rhode, W., 26th ICRC, HE.3.1.07, Salt Lake City, 1999
2. Chirkin, D., Rhode, W., 27th ICRC, HE 220, Hamburg, 2001
3. Chirkin, D., Rhode, W., Proceedings of 2nd Workshop on Methodical Aspects of Underwater/Underice Neutrino Telescopes, Hamburg, 2001
4. Chirkin D. 2003, Ph.D. thesis, UC Berkeley, in preparation
5. Hörandel, J., Astropart. Phys. 19 (2003) 193
6. Hundertmark, S., DESY-PROC-1999-1, 276, 1999
7. Rhode, W., Cârloganu, C., DESY-PROC-1999-01, 1999
8. Wagner, W., et al., this volume
9. Wiebel-Sooth, B. & Biermann, P.L. 1999, Landolt-Bornstein, vol. VI/3c, Springer Verlag, 37